Iranian Journal of Materials Science and Engineering, Vol. 20, Number 1, March 2023
RESEARCH PAPER

The Comparison of Effects of Ultrasonic Treatment, SIMA Process and Al-5Ti-1B Grain Refiner on the Microstructure and Mechanical Properties of Al–15%Mg_2Si In-Situ Composite

Mohammad Alipour

* *alipourmo@tabrizu.ac.ir*

Faculty of Mechanical engineering, Department of Materials Engineering, University of Tabriz, Iran

Received: August 2022 **Revised: March 2023** **Accepted: March 2023**
DOI: 10.22068/ijmse.2957

Abstract: *The effect of strain-induced melt-activated (SIMA) process, ultrasonic treatment (UST) and Al-5Ti-1B refiner on the microstructure and globularity of Al–15%Mg_2Si composite was studied. Deformation of 25% were used. After deformation the samples were heated at 560, 580 and 595°C for 5, 10, 20 and 40 min. The composite was treated with different amounts of the Ti concentrations and ultrasonic treatment with different power. Microstructural study was carried out on the alloy. It was observed that SIMA process, ultrasonic treatment and Al-5Ti-1B refiner has caused the globular morphology of Mg_2Si particles. The results showed that for the desired microstructures of the alloy during SIMA process, the optimum temperature and time were 595°C and 20 min, respectively. Optimum amount of Ti refiner was 1 wt.%, and power for UST was 1800 W. After applying the SIMA process, Al-5Ti-1B master alloy and ultrasonic treatment, the strength and engagement have increased. This means that tensile strength increased from 251 MPa to 303 MPa and elongation percentage improved from 2.1 to 3.4, respectively.*

Keywords: *Deformation, Semisolid, SIMA, Mg_2Si phase, Modification.*

1. INTRODUCTION

Particulate reinforced aluminum metal matrix composites (MMCs) have received a considerable amount of attention in recent years because of their low specific weights [1], high specific tensile strength, high wear resistance, low thermal-expansion, and improved mechanical properties at a wide range of temperatures [2]. These properties of aluminum MMCs make them potential materials in the field of aerospace, automotive and other industries [3, 4].

Al-based composites reinforced with particles of Mg_2Si have been introduced as a new group of composites. These composites have a potential as automobile brake disk material because the Mg_2Si exhibits low density, high hardness, low thermal expansion coefficient and reasonably high elastic modulus [1, 5–8]. However, the mechanical properties of the Al/ Mg_2Si composites are not satisfactory due to the large size of Mg_2Si particles [9]. Therefore, controlling the primary Mg_2Si phase is a key problem for acquiring excellent mechanical properties. In order to modify the shaped Mg_2Si phases in the Al–Mg-Si alloys, many methods have been studied, such as hot extrusion [10, 11], rapid solidification [12], mechanical alloying [13, 14] and micro-alloying (Sb, Ca, and P) [15–17]. But some investigations indicated that these methods may lead to the increase of the production cost and other problems [16].

Semisolid metal (SSM) processing has been developed rapidly since the 1970s [18]. SSM processing is regarded as an advanced forming technology for aluminum and magnesium alloy. The methods to obtain a semisolid structure are mainly electromagnetism stirring, mechanical stirring, spray stirring and semisolid isothermal heat treatment [19]. Comparing with these methods, SIMA has several advantages. It omits the procedure of molten metal treatment, and is applicable for both low and high melting alloys [20-25]. Recent results indicate that the shaped Mg_2Si phases in Mg–6Al–1Zn–0.7Si alloy can be modified to granule and/or polygon shapes by semisolid isothermal heat treatment [26]. Previous research shows [27] that the eutectic Mg_2Si phase changes from the initial shape to granule and/or polygon shape in Mg–9Al–1Si alloy during the isothermal heat treatment. But less work has been done on the Al– Mg–Si alloy by the SIMA process.

In the present work, the effect of ultrasonic treatment, SIMA process and Al-5Ti-1B master alloy on the microstructure and mechanical

[DOI: 10.22068/ijmse.2957]

properties of Al–15%Mg_2Si in-situ composite was studied.

2. EXPERIMENTAL PROCEDURE

Industrially pure elemental Al, Mg and Si were used as starting materials to prepare Al–9.5%Mg–5.5% Si master alloys (all the compositions given in this paper are in wt.%), which corresponds to a composition of Al–15%Mg_2Si. All the alloys were heated in an electrical resistance furnace. Mg was added into the melt with an extra of 20% of the target composition in order to balance the oxidation loss. The composition of this alloy is in hypereutectic region, as shown in Fig. 1 [5].

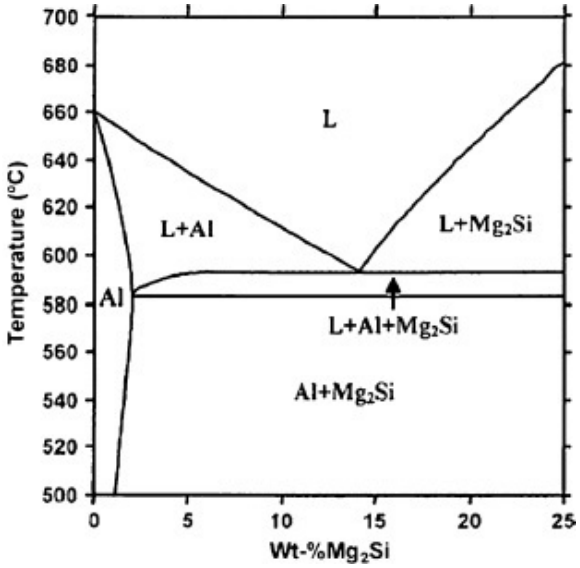

Fig. 1. Calculated equilibrium Al-Mg_2Si phase: pseudoeutectic point at Al-13.9% Mg_2Si. [5].

Primary Mg_2Si crystals were produced in situ during the solidification process. The parent ingots were cut in small pieces then were remelted at 750°C. Degassing was conducted by submerging dry C_2Cl_6 containing broken tablets. Prior to casting, the melt was treated with different amounts of the Ti concentrations. The added values were 0.1, 0.2, 0.6, 1 and 2 wt.% Ti for Al–5Ti–1B grain refiner. After stirring and skimming off the dross, the alloys were poured into a permanent mold prepared according to ASTM B108 standard (Fig. 2). Specimens for microstructural studies were cut from a standard location on the ingots at 25 mm from the bottom of the castings. The modified strain-induced melt activation (SIMA) process was applied to the as-cast before microstructural studies. For the modified SIMA process (Fig. 3), the cylindrical cast specimens were homogenized at 460°C for 24 h and then they were quenched in water (25°C). After reheating the homogenized specimens to 300°C, warm deformation was conducted by a 400 ton hydraulic press. For all specimens, a constant deformation (25%) was selected to provide adequate strain in SIMA process. The deformed samples were then heated to various temperatures within the range of the 550-600°C and maintained at those temperatures for various holding times (5–40 min) as listed in Table 1 [18, 19].

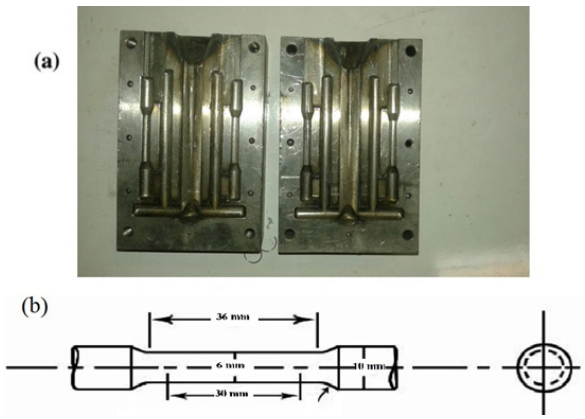

Fig. 2. Tensile specimen geometry and dimensions (a) cast iron mold and (b) tensile sample dimensions.

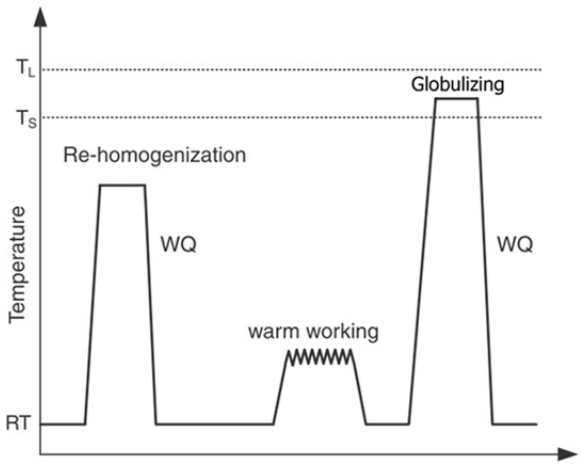

Fig. 3. Schematic illustration of SIMA process.

A schematic of the ultrasonic treatment equipment shown in Fig. 4. The setup consists of 20 kHz-2000 W ultrasonic generator, transducer, a cylindrical Ti probe, a control panel (for power and frequency adjustments) and an electrical resistance furnace that is used to melt the Al–15% Mg_2Si composite. The melt temperature is

[DOI: 10.22068/ijmse.2957]

measured by a k-type thermocouple. The furnace was heat up to 750°C when the Al–15% Mg_2Si composite ingot melts. Then move the probe into the melt. A 500 W, 1000 W and 1800 W power (about 90% of the maximum available power 2 kW) was applied to the melt via a Ti probe for 10 minutes during solidification. The melt surface was protected by argon gas. The UST samples were obtained by treating the melt with degassing at 750°C, and then pour it into the metal mold at 750°C.

Table 1. The heat treatment conditions of warm-worked alloys for SIMA process.

Temperature (◦C)	Time (min)	Predeformation (%)
560	5	25
560	10	25
560	20	25
560	40	25
580	5	25
580	10	25
580	20	25
580	40	25
595	5	25
595	10	25
595	20	25
595	40	25

For microstructural studies, both an optical microscope equipped with an image analysis system (Clemex Vision Pro. Ver.3.5.025) and scanning electron microscope performed in a Cam Scan MV2300 SEM, equipped with an energy dispersive X-ray analysis (EDX) accessory have been used. The cut sections were polished and then etched by Keller's reagent (2 ml HF, 3 ml HCl, 5 ml HNO_3 and 190 ml H_2O) to reveal the structure. Tensile testing on all the composite samples was performed at room temperature using KOOPA universal testing machine at the strain rate of 1 mm/min. Four test bars were tested for each composite sample and the average value is reported here.

3. RESULTS AND DISCUSSION

3.1. Microstructural Study

Fig. 5 shows the microstructure of the as-cast Al-15Mg_2Si composite before and after deformation. As seen from Fig. 5a, the as-cast microstructure of Al-15Mg_2Si composite contains three constituents: white primary α-Al dendrites, Chinese script Mg_2Si particles and pseudo-eutectic matrix respectively. Fig. 5b shows 25% deformation which clearly exhibits heavily oriented α_{Al} dendrites in the direction that was vertical to the warm working direction; especially a fragment of Mg_2Si occurs due to its brittleness. During plastic deformation of samples, internal strain energy is stored in the form of dislocation multiplication, elasticity stress and vacancies, which provide the driving force for recovery and recrystallization.

Figs. 6, 7 and 8 show the microstructures of Al-15Mg_2Si composite specimens after applying different holding time and holding temperature during SIMA process. The α_{Al} grain size and Mg_2Si particle size are very important. From Figs. 6, 7 and 8, it is clear that the fine and uniform structures are related to Fig. 7d and 8d with 40 min holding time at 580°C and 595°C.

Figs. 6, 7 and 8 show the morphology of the Mg_2Si phase in semisolid microstructures of Al-15 Mg_2Si composite with 25% reduction ratio after heat treatment at 560, 580 and 595°C for 5, 10, 20 and 40 min. It is observed that the original shaped Mg_2Si is fragmented (as shown in Figs. 6, 7 and 8), with the morphology of rounded-corner shape, instead of polygon shape during semisolid heat treatment, and Mg_2Si particles size has been reduced. Thus the morphology of Mg_2Si phases in the experimental alloy changes from the initial polygonal shape to granule and/or polygon shapes. However, M. Zha et al. [28] reported that the eutectic Mg_2Si in Mg–5Si–1Al alloy turns from granular shape into Chinese script morphology by partial remelting owing to the low Al content with increasing liquid volume fraction above 660°C. In spite of the above, the modification mechanism of Chinese script shaped Mg_2Si phases during the SIMA process is not completely clear, and further investigation needs to be carried out.

Fig. 9 shows the morphology of the Mg_2Si phase in semisolid microstructures of Al-15 Mg_2Si composite with 25% reduction ratio after heat treatment at 560, 580 and 595°C for 20 min. From Fig. 10, it can be seen that the minimum average Mg_2Si particles size for Al-15Mg_2Si composite is 20 μm. It is expected that at shorter holding times, only a small quantity of the eutectic phase melts and as the time proceeds to longer times, most of the eutectic located at the boundaries of primary phase melts. Primary

[DOI: 10.22068/ijmse.2957]

Mg_2Si particles when formed during solidification cause the formation of germination centers for dendrites and change the structure of dendrites. With the presence of titanium in the structure. Because the number of Mg_2Si particles per unit volume increases, the effect of Mg_2Si particles on the structure of dendrites will be doubled.

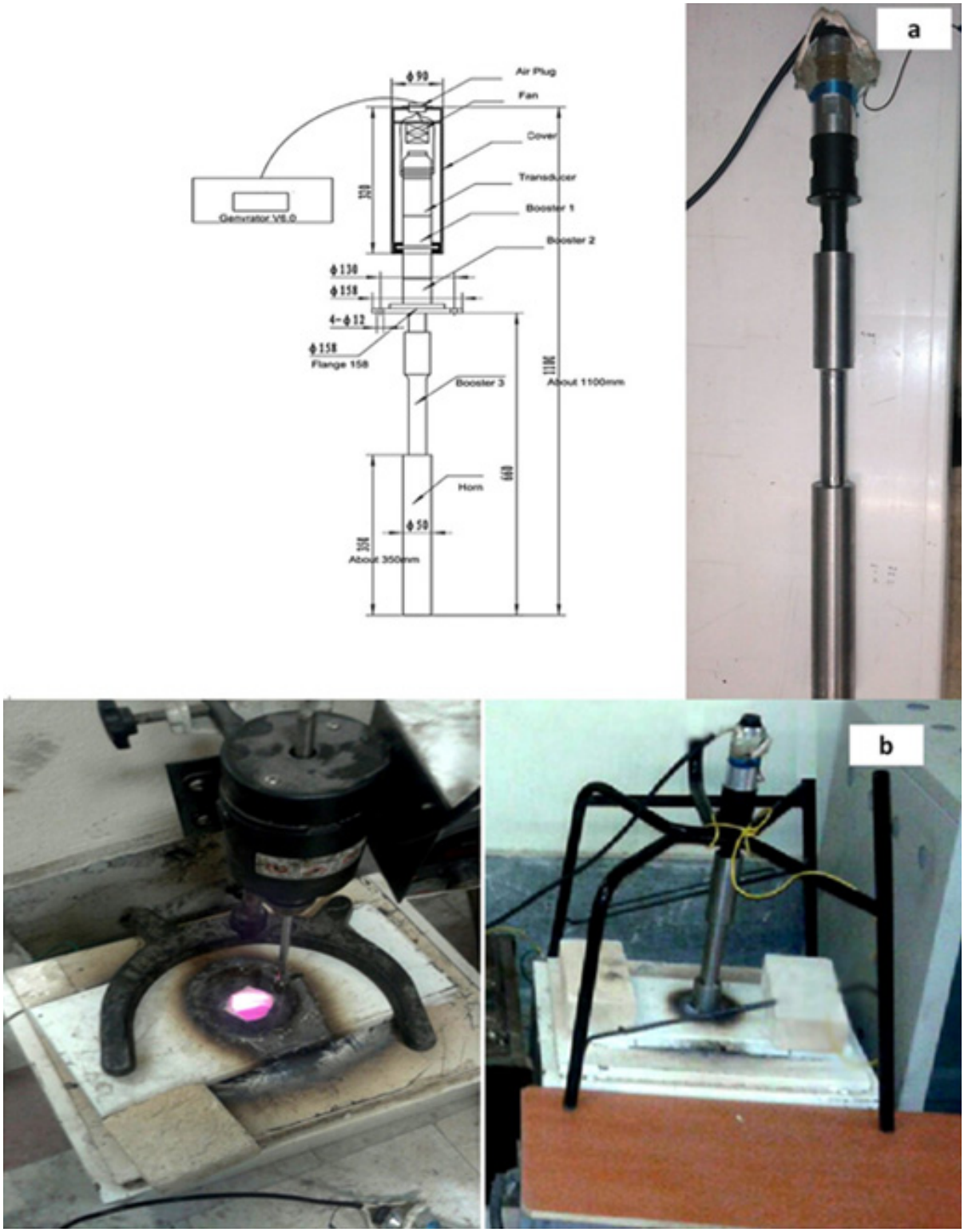

Fig. 4. a) Ultrasonic probe and (b) mechanical stirrer and ultrasonic device.

[DOI: 10.22068/ijmse.2957]

Generally, SIMA is considered a process in which the basic forged, extruded or rolled bars are subjected to additional deformation to accumulate a large quantity of deformation energy for inducing sufficient strain, and then heated to the semi-solid condition to transform the dendritic structure to a fine, uniform and spheroidal microstructure.

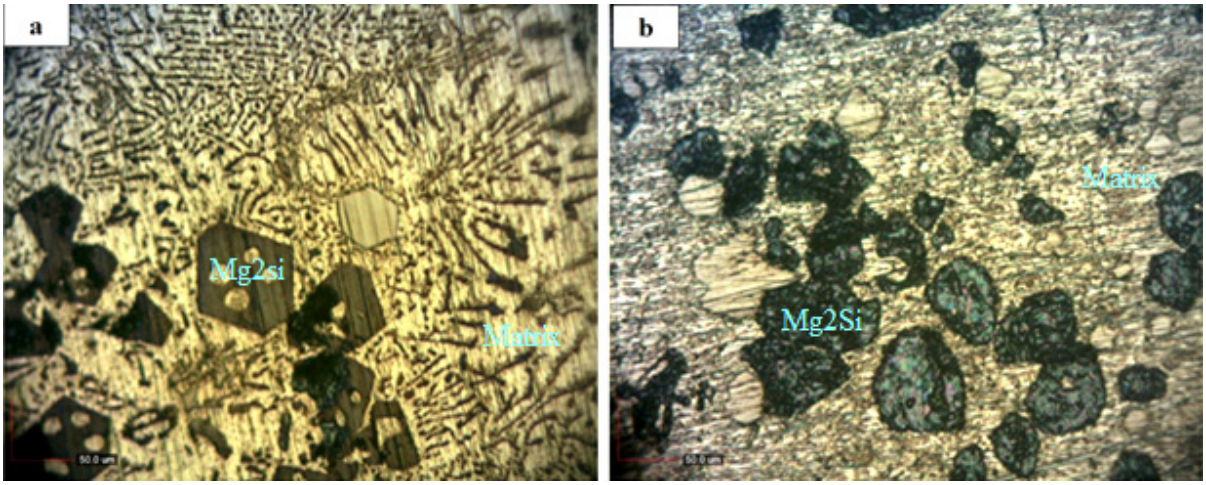

Fig. 5. Optical micrographs of cast Al-Mg_2Si composite (a) as cast and at 25% deformation in 300°C.

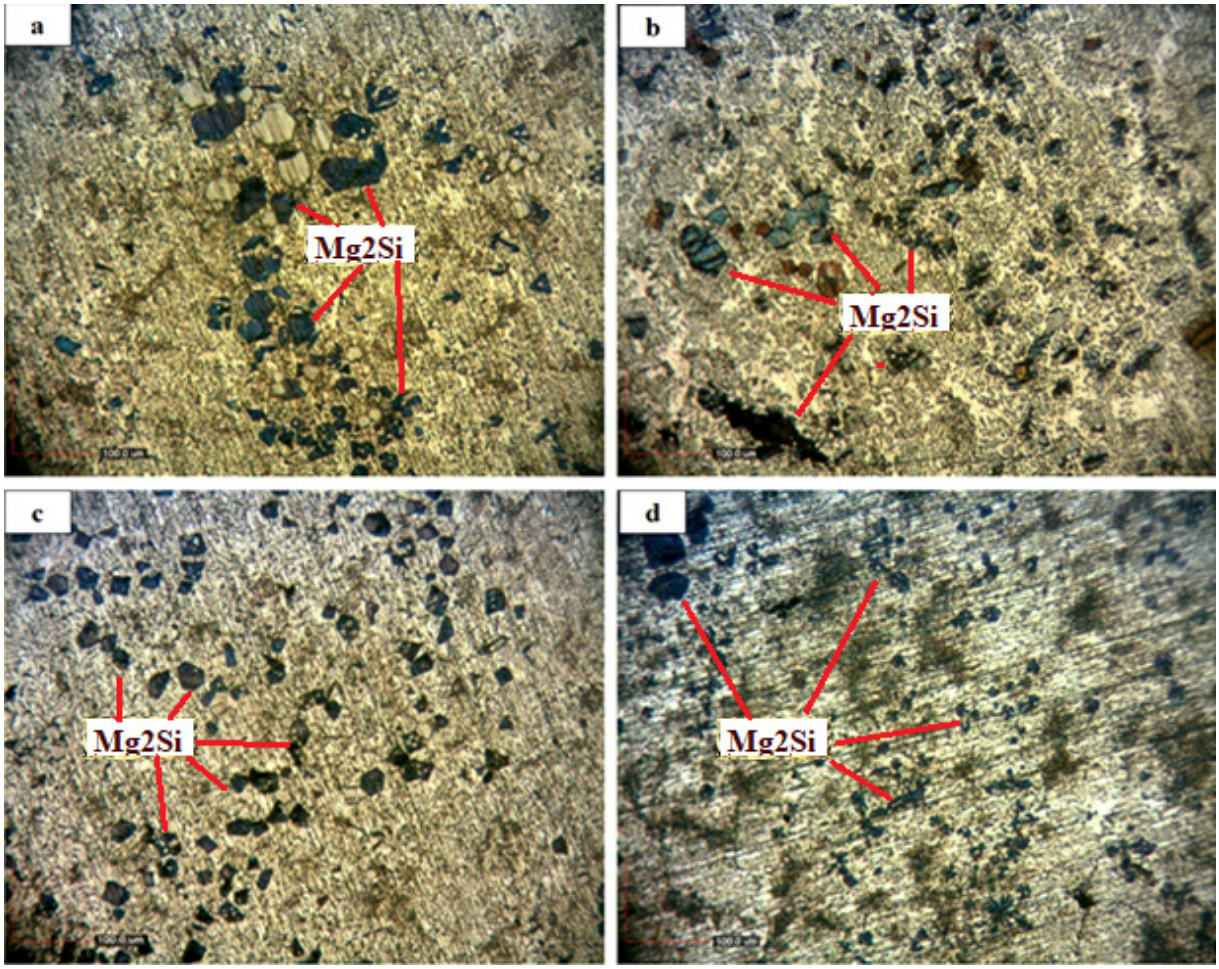

Fig. 6. Microstructures of 25% deformed after holding at 560°C for (a) 5 min, (b) 10 min, (c) 20 min and (d) 40 min for Al-15Mg_2Si composite.

[DOI: 10.22068/ijmse.2957]

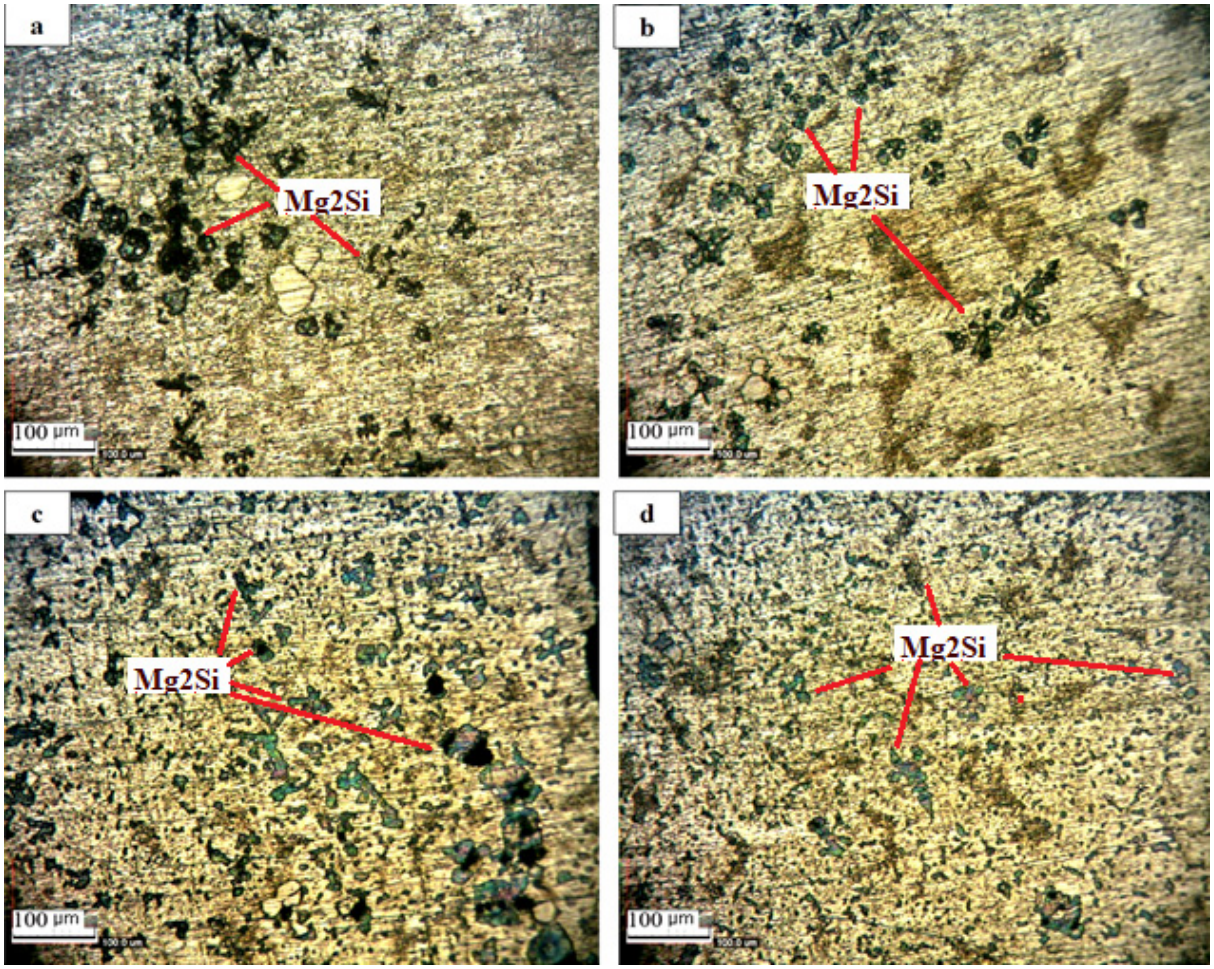

Fig. 7. Microstructures of 25% deformed after holding at 580°C for (a) 5 min, (b) 10 min, (c) 20 min and (d) 40 min for Al-15Mg_2Si composite.

The deformation energy accumulated by increasing dislocation density is closely related to the deformation process. It was well showed that in SIMA process increasing the heat treatment temperature increases the amount of liquid within dendrite arm spacing. Due to the effects of surface tension and interface curvature, the convex edges of the dendrites melt and decrease the interface area of the dendrites leading to a lower free energy. Moreover, the concentration of the solute in the concave parts of the dendrites is higher, which increases the amount of liquid in these areas.

When the liquid of the two concaves contacted with each other, the dendrites would separate into autonomous small dendrites. It should be noted that increasing the heat treatment temperature causes a further dissolution of eutectics and spheroidization of the α-Al dendrites. At temperatures more than the eutectic temperature, the eutectic phase dissolves completely and the atoms diffuse to the α-Al dendrites due to increasing of the diffusion capacity and the solubility of the elements in α-Al at higher temperatures [29]. It was resulted that the structure of dendrites should gently become irregular with decreasing holding time. At the deformation stage, the samples accumulated enough deformation energy at the boundaries of dendrites and subdendrites to provide the kinetic of partial remelting. When the samples were heated to the semi-solid temperature, melting would occur at these boundaries and novel dendrites appeared.

With increasing holding time, the structure of these grains became bigger and more spheroidal. Under the condition of long holding time, the dendrites coarsened due to the mechanisms of coalescence and Ostwald ripening [30, 31].

[DOI: 10.22068/ijmse.2957]

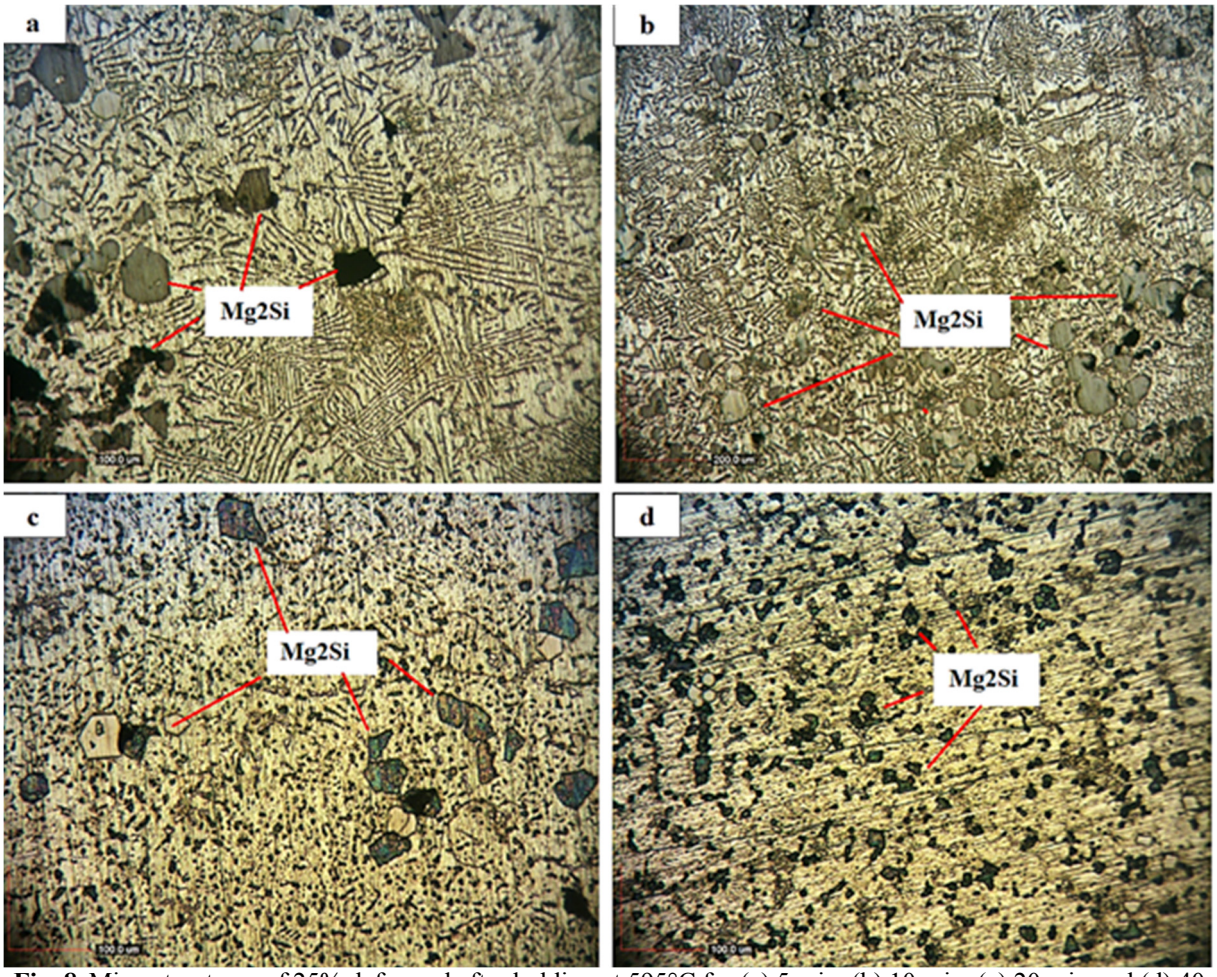

Fig. 8. Microstructures of 25% deformed after holding at 595°C for (a) 5 min, (b) 10 min, (c) 20 min and (d) 40 min for Al-15Mg_2Si composite.

The microstructure evolution to spheroidal structure was promoted by the reduction of the area of interface between the solid and the liquid phase. Clearly, enough holding time ensured the complete evolution of the microstructure. The fine and spheroidal dendrites could only be acquired if the intellectual holding time was selected. The experiment provides witness that supports the deformation-recrystallization mechanism proposed by Doherty et al. [32] as the main mechanism responsible for the formation of the spheroidal microstructure via the SIMA process.

There are two steps for the SIMA process. The first step is plastic deformation below solidus temperature for the material with a dendrite structure. This is accomplished usually by hot rolling or cold rolling or/and then by upsetting to increase the amount of plastic deformation.

The second step is to rapidly heat the material to a temperature between the solidus and liquidus. In the first step, the microstructure will change in the follow steps: (1) when the plastic deformation is small, in addition to slip and cross-slip in which dislocations move and cause material to deform, twinning will be aroused by the load [33]; (2) there will appear new grain boundaries where the atoms are not properly spaced as shown in Fig. 11b; (3) for higher levels of deformation, the grains rotate and elongate, as shown in Fig. 11c; (4) when grains (single crystal) elongate, they will be break up as step (1), which is shown in Fig. 11d.

The microstructure evolution for the first step can be verified [34]. In the second step, the material is heated to the temperature between the solidus and liquidus where the interdendritic spaces has more energy will melt first, and the dendrites gradually change to a rounded shape.

[DOI: 10.22068/ijmse.2957]

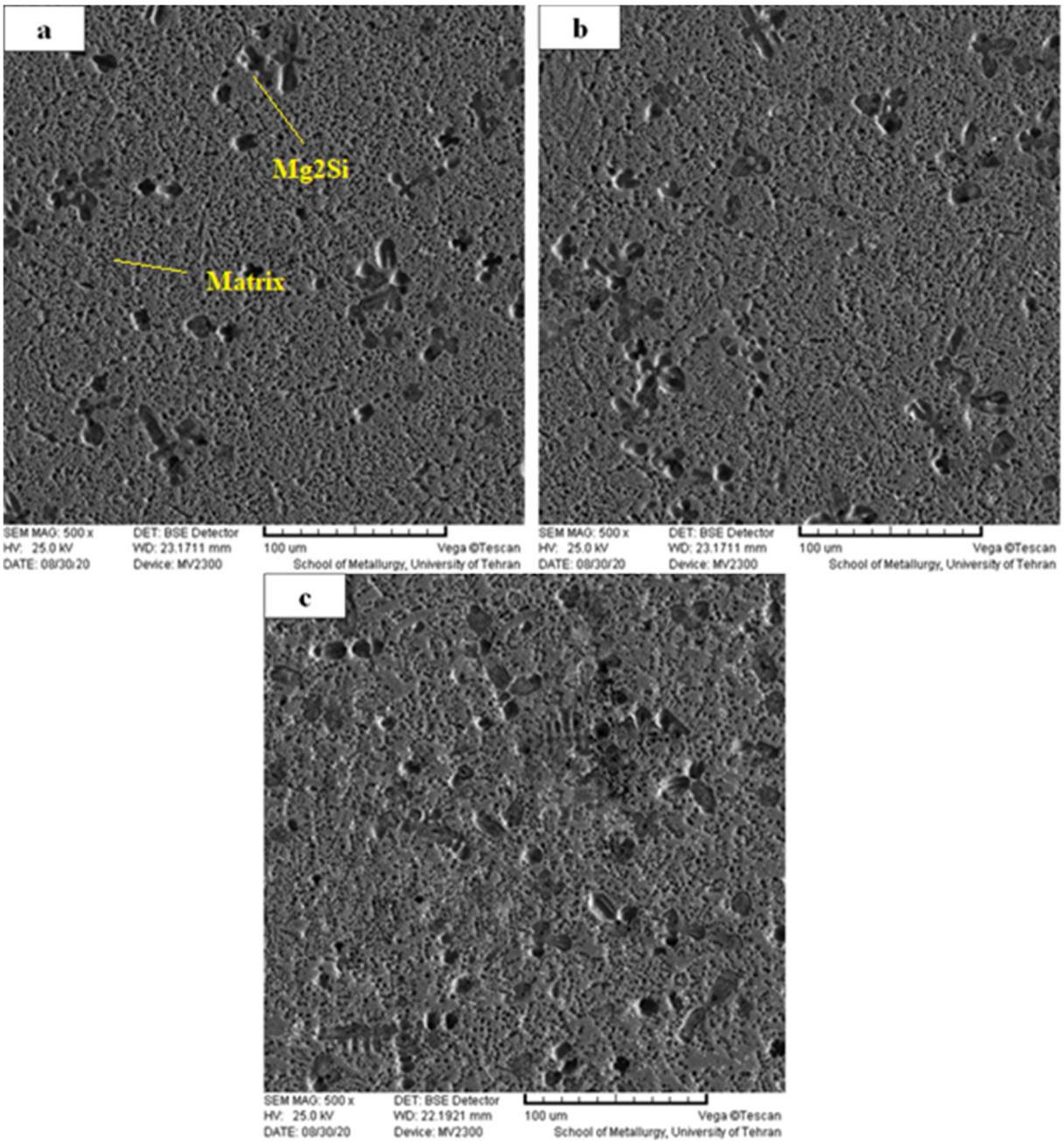

Fig. 9. Microstructures of 25% predeformed and holding time 20 min held at 560°C (a), 580°C (b) and 595°C (c) for unrefined alloy.

In order to explain this phenomenon, we may cite the relationship between surface curvature of the dendrite and the decrease in equilibrium melting point [35]. Coalescence and Ostwald ripening mechanisms [36] play an important role to increase the average size of the α_{Al} particles. The coarsening mechanism is the coalescence of α_{Al} grains, which occurs between adjoining dendrites at low liquid fraction. Liquid content plays an important role in kinetics of coalescence since it defines the number of solid necks between dendrites. It has been shown that the coalescence frequency is proportional to the number of adjacent dendrites. Therefore, coalescence is expected to occur at early stages of heating or in high fraction solid in the semi-solid regime where the number of necks per dendrite is relatively high and grains are discrete. Ostwald ripening involves the growth of larger αAl particles at the expense of smaller αAl particles, and it is governed by the

[DOI: 10.22068/ijmse.2957]

Gibbs–Thompson effect. This effect changes the chemical potential of solutes at the particle/liquid interface, depending on the curvature of the interface [36]. The lowering of interfacial energy between the solid phase and liquid phase supplies the driving force for grain coarsening. The larger grain gradually becomes spheroidal to lower the solid/liquid interfacial energy. Ostwald ripening is active at higher liquid fraction, in which αAl grains continuously coarsen and the small grain gradually melts. The isothermal holding time, temperature and degree of predeformation have effects on the average size and degree of spheroidization of α_{Al} particles of semi-solid slurry.

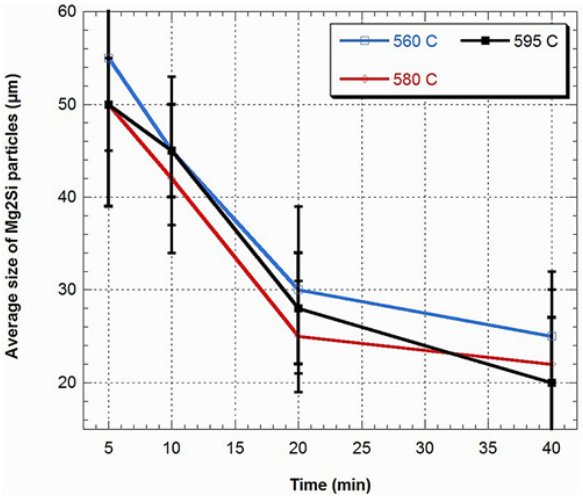

Fig. 10. Variations of average Mg_2Si particles size before and after SIMA process with holding time in 560, 580, 595°C after a 25% deformation for Al-15Mg_2Si composite.

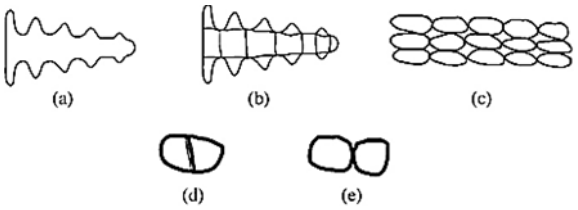

Fig. 11. Illustration of microstructure evolution model for SIMA: (a) dendrite arm, (b) dendrite arm after small deformation, (c) microstructure after grain rotation and elongation, (d) grain interior after elongation, (e) break-up of grains.

Fig. 12 depicts the underling behavior of Mg_2Si and α- Al particles during the heat treatment. Dissolution of last solidified phases with low melting point occurs during the initial stages of heat treatment. The boundaries of these original phases, which were formed due to segregation, are further penetrated by the surrounding melt in a temperature above the solidus (Fig. 12(b)). Dendrite arms are then remelted at their roots which lead to normal ripening of dendrite arms (Fig. 12(c)). At next step, the fragmented arm renders to a spheroidal or ellipsoidal grain (Fig. 12(d)). It is obvious that the size of this new grain is dependent on the size of its original dendrite arm. At next step and in case of short spacing between ripened dendrite arms, joining of adjacent particles occurs, and as a result a little amount of liquid known as "Liquid Islands" will be entrapped inside the yielded grain which is also identified as a new globular grain (Fig. 12(e)). When continue heating until semi-solid temperature and holding for a predetermined time, it also evolves toward spheroidal morphology [37].

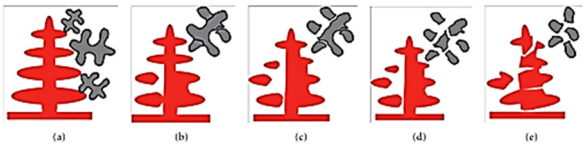

Fig. 12. Schematic illustration of semisolid structure evolution during heat treatment of (a) original dendrites, (b) and (c) melting, liquid penetration and combining, (d) removing and € coalescence, ripening and spheroid formation [37].

Fig. 13 shows the Al-15Mg_2Si composite as-cast microstructures after ultrasonic treatment. The samples without UST (ultrasonic treatment) have coarser microstructures than the ones with UST. What's more important, the dendrite structure is mostly eliminated. When comparing Fig. 13 and 3(a), it can be seen that the Mg_2Si (black area) is slightly refined. This is another important effect of UST. The microstructures (in particular, the Mg_2Si phase) processed under UST are more refined when compared with the standard alloy. And the secondary phase, which is Mg_2Si, is refined due to Fig. 13(a) (b) (c). Ultrasonic treatment can reduce the size of eutectic and Mg_2Si by over an order of magnitude; the aspect ratio was also reduced by ultrasonic treatment.
But, high power acoustic energy was injected into the melt, which should result in slower growth rate of eutectic and Mg_2Si phases. There should be other causes. Many other phenomena that occur during ultrasonic processing of alloy may contribute to the refinement of the eutectic and

[DOI: 10.22068/ijmse.2957]

Mg_2Si phase. One phenomenon is ultrasonic induced convection. The strong convection may enhance the heat transfer from the melt to the environment, which will definitely increase the cooling rate of melt. And because of that, samples treated by ultrasonic may have higher eutectic and Mg_2Si phase's growth rate. Acoustically induced convection can also affect nucleation of the eutectic and Mg_2Si phases by altering the constitutional supercooling at the front of the growing eutectic grains. Another phenomenon is the ultrasonic induced pressure oscillations in the liquid pools. Further research is still needed to determine the effect of this phenomenon on the growth of eutectic and Mg_2Si pheses.

Fig. 14 shows SEM back scattered images of Al-15Mg2Si composite in as-cast condition in Ti-refined alloys. It is noticeable that grain refinement by Al-5Ti-1B enhances the number of grain boundaries and promotes a more homogeneous distribution of intermetallic compounds and eutectic structure [38]. Fig. 14 also illustrates the changes in dendrite morphology of the Al-15Mg_2Si composite after addition of 1 wt.% Ti. Fig. 15 shows SEM back scattered images of Al-15Mg_2Si composite in high magnification.

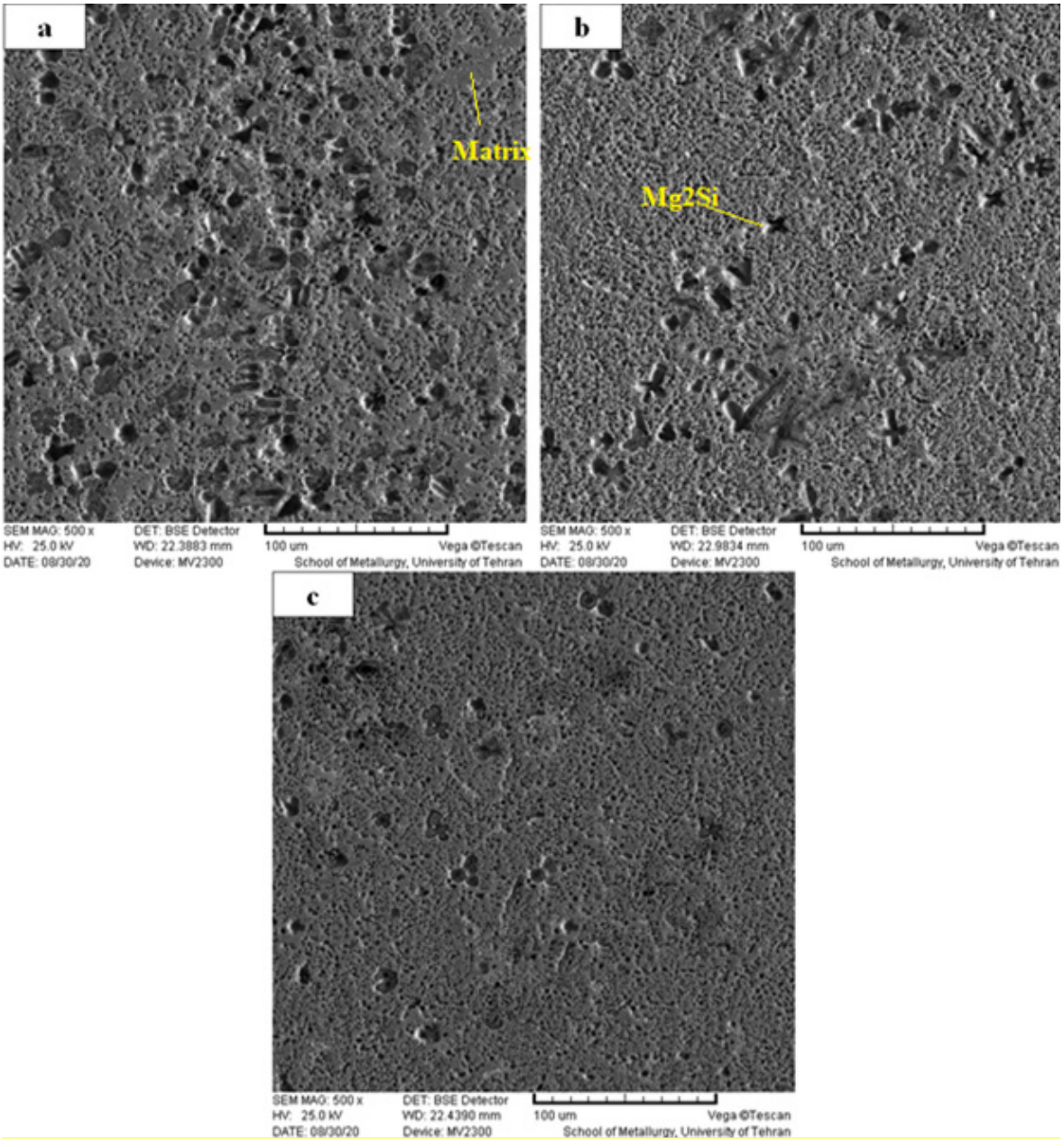

Fig. 13. Microstructures of refined specimens, with ultrasonic waves (a) 500 W, (b) 1000 W and (c) 1800 W.

[DOI: 10.22068/ijmse.2957]

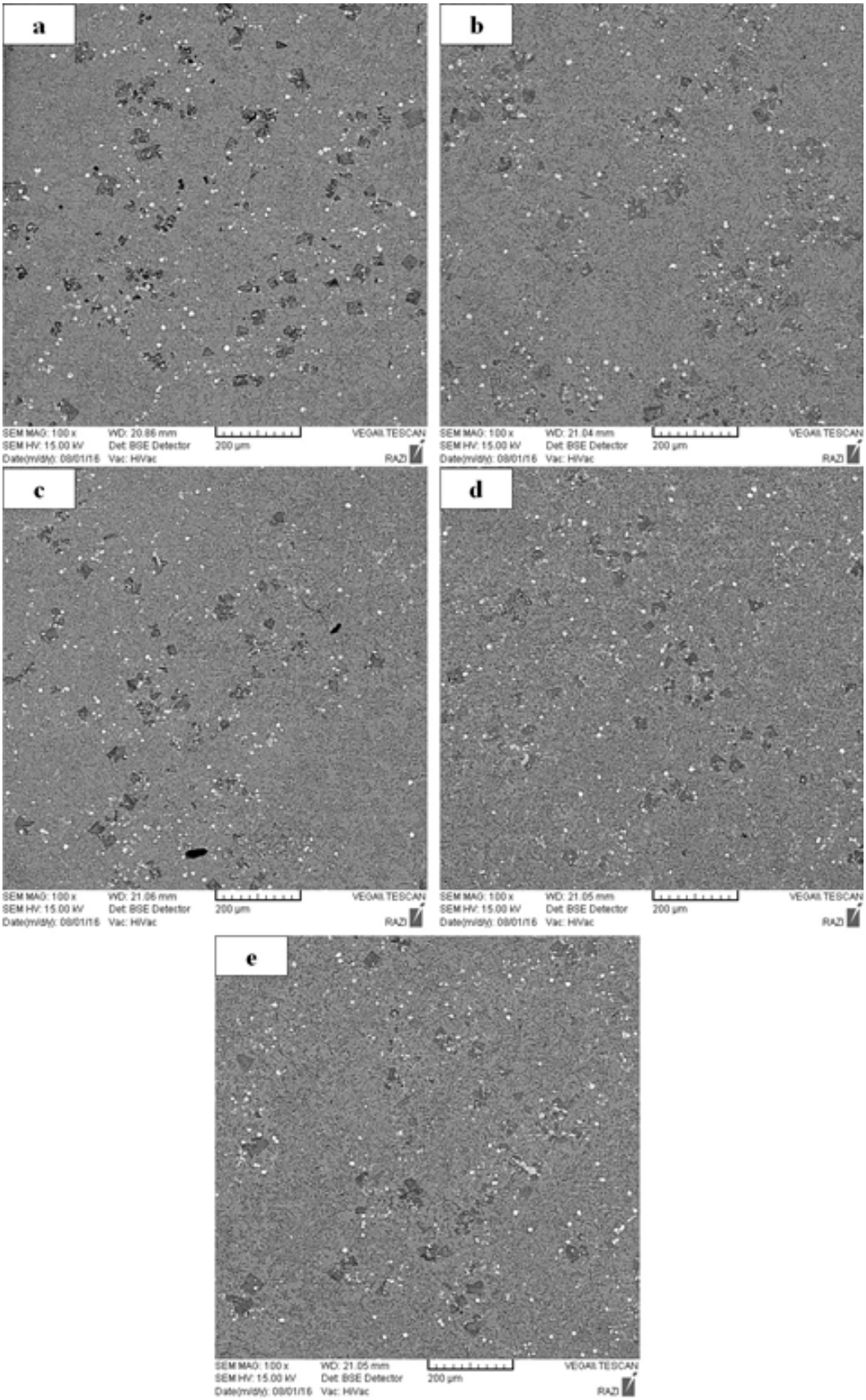

Fig. 14. Microstructures of refined specimens, with (a) 0.1% Ti, (b) 0.2% Ti, (c) 0. 6% Ti, (d) 1% Ti and (e) 2% Ti.

[DOI: 10.22068/ijmse.2957]

To obtain an appropriate combination of refined structure, it was necessary to find optimum levels of the applied refiners. From Fig. 14 and tensile result, the optimum level of Ti was found to be 1 wt.%. Several mechanisms have been proposed for the grain refining process [39]. In some mechanisms the presence of some particles like $TiAl_3$, TiB_2 and AlB_2 are known to be effective for grain refinement procedure. In comparison with AlB_2 and TiB_2, $TiAl_3$ is known to be a potent nucleating site for aluminum [40]. From Fig. 14, two microstructural changes can be observed: (1) With Ti addition, the average size of Mg_2Si particles decreased. (2) The morphology of the Mg_2Si primary particles changed from an irregular shape to the faceted polygonal. The exact mechanism for changes in the morphology of particles is not clear. This effect might be either by increasing the melting entropy of Mg_2Si particles or by changing the surface energy of Mg_2Si crystals by lattice distortion due to the existence of Ti in the Mg_2Si lattice. Fig. 16 shows the results from the map analysis in the refined sample. The segregation of solute occurred during solidification of the alloy. Fig. 16 shows that titanium-containing compounds are evenly distributed in the composite matrix.

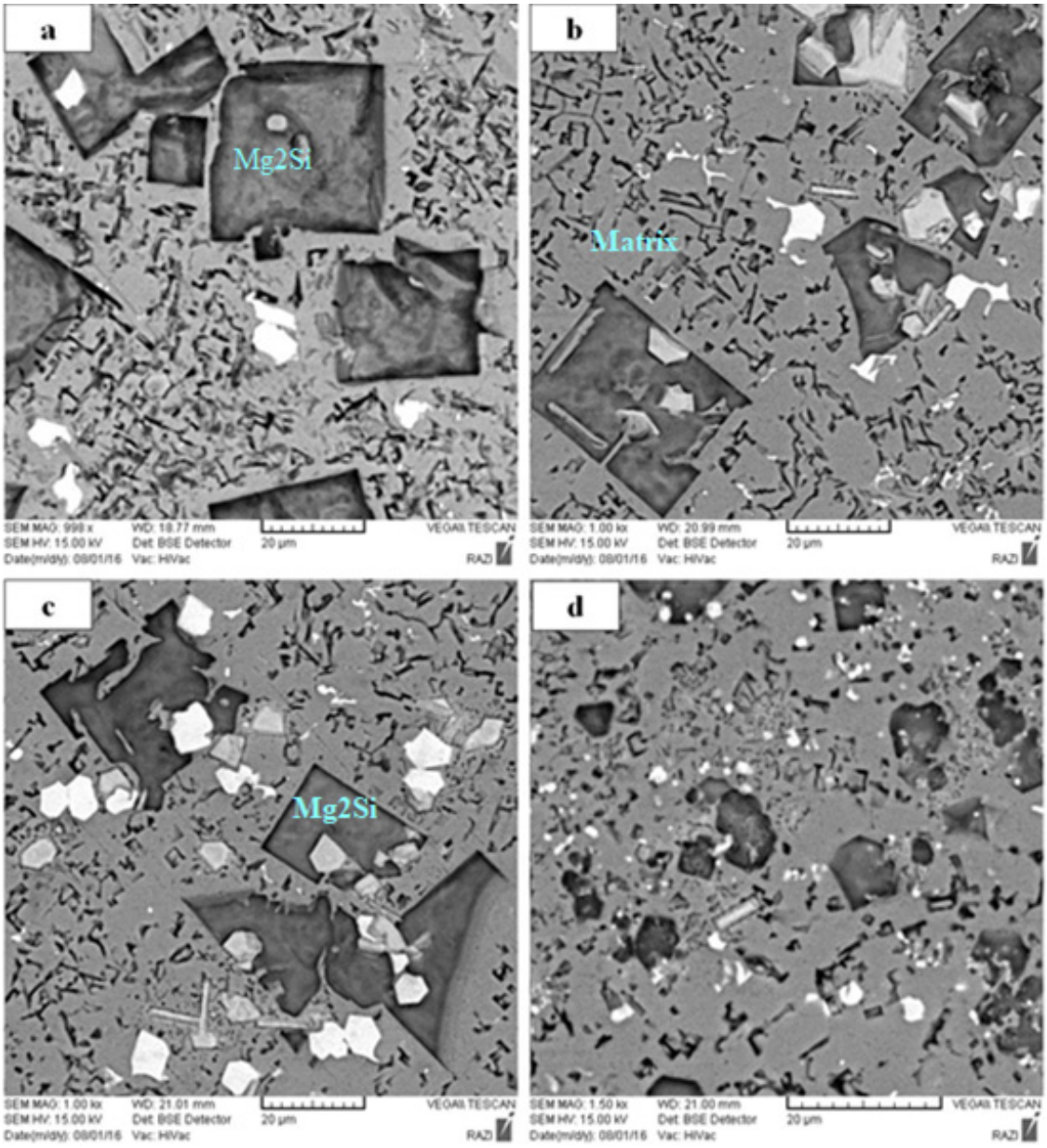

Fig. 15. Microstructures of refined specimens, with (a) 0.1% Ti, (b) 0.2% Ti, (c) 1% Ti and (d) 2% Ti in high magnification.

[DOI: 10.22068/ijmse.2957]

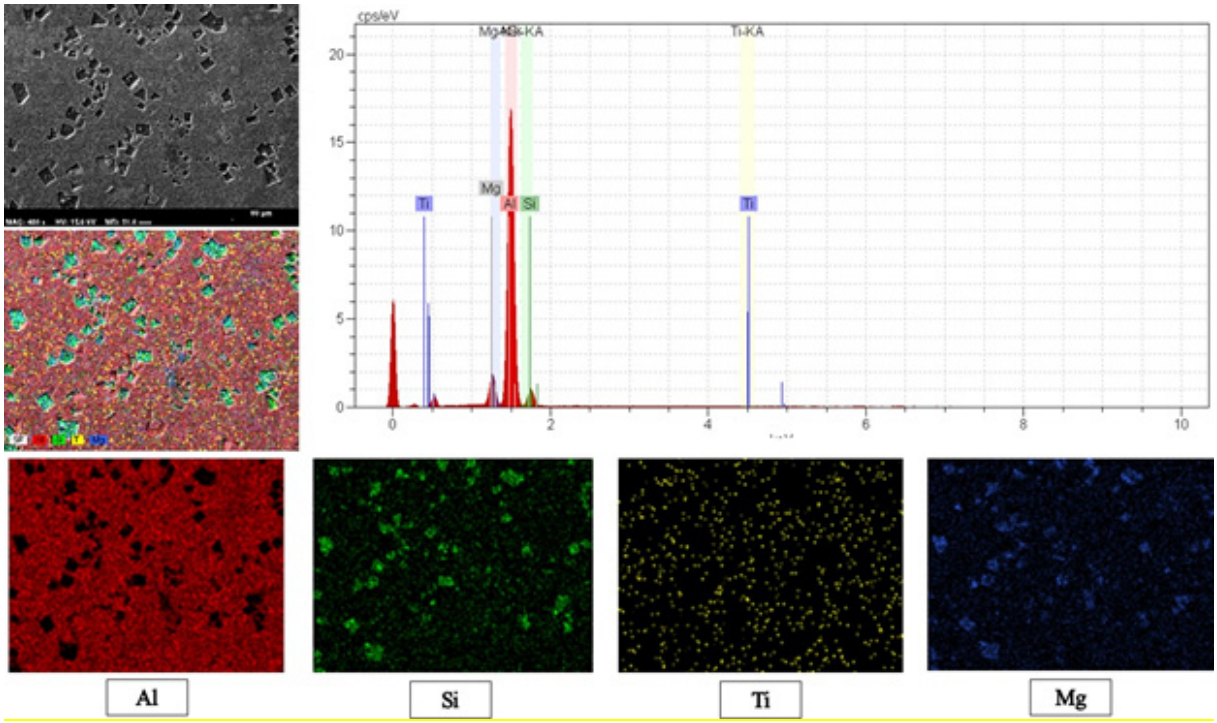

Fig. 16. X-ray energy spectrums of the structure and distribution of the major elements in structure by SEM and map analysis in sample refined by 1% Ti.

3.2. Tensile Properties

Tab. 2 shows UTS and elongation values of Al–15%Mg_2Si composite before and after SIMA process, ultrasonic treatment (UST) and adding Ti refiner. It is evident that the cast material shows poor UTS and elongation response as the value is far low (2.1%) and minor addition of Ti, i.e. 0.1 wt%, enhances the ductility beyond which up to 1 wt.% Ti both UTS and elongation values of the composite are improved. Also, after applying the SIMA process and applying ultrasonic treatment, the strength and engagement have increased.

This means that tensile strength increases from 251 MPa to 303 MPa and elongation percentage improves from 2.1 to 3.4, respectively. According to the results, it seems that the tensile properties of the samples are under influence of different factors between which the competition is governed by the resultant property. By the addition of Al-5Ti-1B, applying the SIMA process and ultrasonic treatment, the microstructural features show a great change in the morphology of secondary Mg_2Si phase in eutectic region.

Microstructural study showed that the morphology of pseudo-eutectic Mg_2Si inside the solidification cell is more flake-like and less fibrous. Similar modification effect of Ti on the eutectic Mg_2Si phase has been reported in Mg-5wt.% Si alloy in as-cast condition [40]. But at higher Ti contents, more intermetallics are seen in the solidification cell as a result of such phenomena.

The formation of AlTi intermetallic particles which are normally hard and brittle can directly influence the UTS and elongation results. By adding 2 wt.% Ti to the composite, no improvement effect is observed in the UTS and elongation results. This is most probably due to the higher concentration of Ti on the last solidification stage and the presence of higher contents of intermetallics in eutectic cells. According to the results, the optimum tensile property is achieved by applying the ultrasonic treatment to the Al-Mg_2Si composite.

According to Griffith's theory, the fracture stress of a composite increase with decreasing of particle size, in inverse proportion to the square root of the particle size. Thus the refined structure has a higher fracture stress, as it has been confirmed by other works in Al–Mg_2Si composites [38, 42, 43, 44, 45]. Smaller particles do not show any holes, which are preferable sites for crack initiation, and are surrounded by the soft alpha phase.

[DOI: 10.22068/ijmse.2957]

Table 2. The results of tensile and elongation of specimens.

properties	σuts (Mpa)	Elongation (%)
Al-15%Mg_2Si	252±16	2.1
Al-15%Mg_2Si-SIMA-560°C-5 min	255±16	2.1
Al-15%Mg_2Si-SIMA-560°C-10 min	263±12	2.3
Al-15%Mg_2Si-SIMA-560°C-20 min	275±14	2.7
Al-15%Mg_2Si-SIMA-560°C-40 min	270±17	2.6
Al-15%Mg_2Si-SIMA-580°C-5 min	262±16	2.1
Al-15%Mg_2Si-SIMA-580°C-10 min	265±12	2.4
Al-15%Mg_2Si-SIMA-580°C-20 min	279±14	3
Al-15%Mg_2Si-SIMA-580°C-40 min	272±17	2.8
Al-15%Mg_2Si-SIMA-595°C-5 min	262±16	2.3
Al-15%Mg_2Si-SIMA-595°C-10 min	270±12	2.6
Al-15%Mg_2Si-SIMA-595°C-20 min	286±14	3.3
Al-15%Mg_2Si-SIMA-595°C-40 min	275±17	2.9
Al-15%Mg_2Si-UST-500 W	280±16	2.8
Al-15%Mg_2Si-UST-1000 W	289±12	3.2
Al-15%Mg_2Si-UST-1800 W	303±14	3.8
Al-15%Mg_2Si-0.1 wt.% Ti	257±17	2.3
Al-15%Mg_2Si-0.2 wt.% Ti	265±16	2.5
Al-15%Mg_2Si-0.6 wt.% Ti	278±12	2.9
Al-15%Mg_2Si-1 wt.% Ti	288±14	3.4
Al-15%Mg_2Si-2wt.% Ti	282±17	3.2

3.3. Fracture Study

Studying fracture characteristics of materials is of prime considerations in the evaluation of their plastic deformation. Fig. 17 shows the scanning electron microscopy fractographs of tensile specimens of the (a) as-cast, (b) SIMA process-595°C- 20 min, (c) refined with 1% Ti and (d) refined with 1800W ultrasonic treatment, respectively. In the cast specimen fractured at room temperature, fracture surfaces are covered by packets with coarse steps, suggesting a brittle mode of failure creating a rapid fracture deriving from their intrinsic brittleness. This appearance is very similar to cleavage fracture, in which some shiny angular flat facets feature a river pattern texture, consistent with the measured total elongations usually observed in cast aluminum alloys at low temperatures. On the other hand, fracture surface in Fig. 17b that modified composite with SIMA process-595°C- 20 min contains several cracked particles together with a few decohered primary Mg_2Si particles. These fine Mg_2Si particles in Al-Mg_2Si can be a barrier to the propagation of cracks and thus enhance the elongation values. As seen, in refined with 1% Ti and refined with 1800W ultrasonic treatment, Fig. 17c-d, dimples present at the fracture surface are rather coarse but homogenous. As known, dimples with honeycomb appearance are characteristics of a semi-ductile mode of fracture.

4. CONCLUSIONS

The effect of SIMA process, Al-5Ti-1B master alloy and ultrasonic treatment on the microstructure and UTS of the Al–Mg_2Si in-situ composites was studied.

The following conclusions can be drawn.

1) Microstructure of the samples prior to the heat treatment was consisted of coarse Mg_2Si phases in a matrix of α-Al and pseudoeutectic cell.
2) The morphology of Mg_2Si particles was dendritic for the sample with 15% of reinforcement. Heat treatment resulted in a finer and globular structure in all samples but was more significant for Al–15% Mg_2Si in 595°C and 20 min respectively.
3) Ultrasonic treatment, SIMA process and Al-5Ti-1B master alloy caused achievement a uniform distribution of Mg_2Si phase in the in-situ composites.
4) After applying the SIMA process, Al-5Ti-1B master alloy and ultrasonic treatment, the strength and engagement were increased. This tensile strength was increased from 251 MPa to 303 MPa and elongation percentage was improved from 2.1 to 3.4, respectively.

[DOI: 10.22068/ijmse.2957]

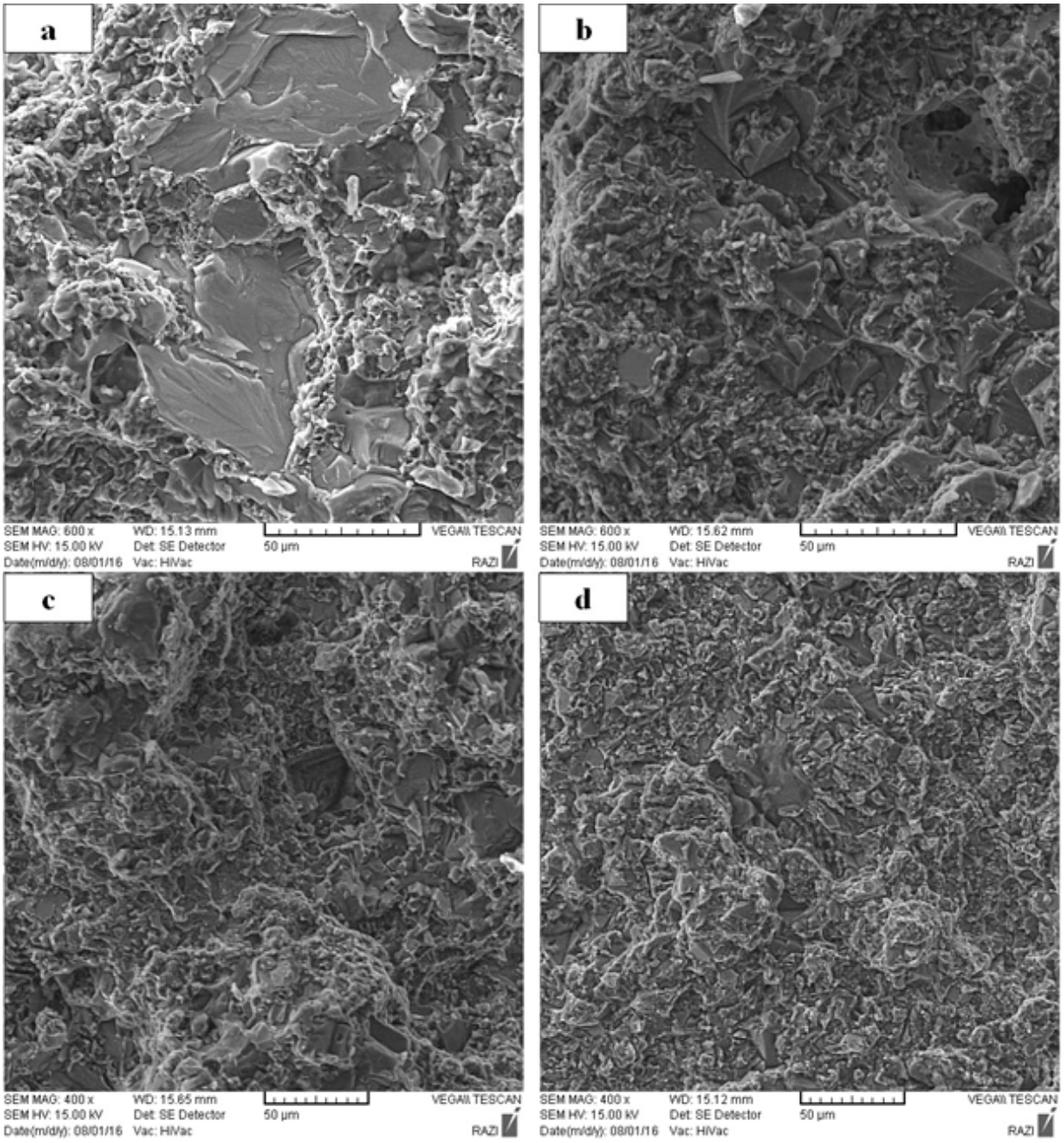

Fig. 17. Secondary electron image of fracture surface related to specimens (a) as-cast, (b) SIMA process-595°C-20 min, (c) refined with 1% Ti and (d) refined with 1800W ultrasonic treatment.

REFERENCES

[1] J. A. Liu, D. Song, L. R. Zhang, X. Z. Yang, X. Y. Zhu, W. B. Sun, F. Y. Chen.," Microstructure and compressive properties of solution heat-treated magnesium-Mg_2Si in-situ composite foams after complex modification." Journal of Materials Research and Technology, 2021, 15, pp 3673-3682.

[2] Wenwen Zhang, Xichao Caoa, Jinyong Zhang, Ji Zoua, Weimin Wang, Qianglong He, Lin Ren, Fan Zhang, Zhengyi Fu.,"B4C-based hard and tough ceramics densified via spark plasma sintering using a novel Mg_2Si sintering aid." Ceramics International, 2023, 49, 145-153.

[3] Hamidreza Ghandvar, Kadhim A. Jabbar, Mohd Hasbullah Idris, Norhayati Ahmad, Muhammad Hafiz Jahare, Seyed Saeid Rahimian Koloor, Michal Petrů.,

[DOI: 10.22068/ijmse.2957]

"Influence of barium addition on the formation of primary Mg_2Si crystals from Al–Mg–Si melts." Journal of Materials Research and Technology, 2021, 11, 448-465.

[4] Li C, Wu Y, Li H, Liu X. "Microstructural formation in hypereutectic Al–Mg_2Si with extra Si.," J Alloys Compd, 2009, 477, 212–216.

[5] Azarbarmas, M., Emamy, M., Karamouz, M., Alipour, M., Rassizadehghani, J., "The effects of boron additions on the microstructure, hardness and tensile properties of in situ Al-15% Mg_2Si composite.," Materials and Design, 2011, 32, 5049-5054.

[6] Azarbarmas, M., Emamy, M., Rassizadehghani, J., Alipour, M., karamouz., "M. The influence of beryllium addition on the microstructure and mechanical properties of Al-15% Mg_2Si in-situ metal matrix composite." Mater Sci Eng A, 2011, 528, 8205-8211.

[7] Azarbarmas, M., Emamy, M., Alipour, M., "Study on fracture behaviour of Al-15% Mg_2Si metal matrix composite with and without beryllium additions." J Mater Sci, 2011, 46, 6856–6862.

[8] Azarbarmas, M., Emamy, M., Rasizadeh, J., Karamouz, M., Alipour, M., "The effects of cooling rate on the microstructure and hardness of Al-15% Mg_2Si in situ composite with Boron." TMS Annual Meeting, 2011, 3, 883-890.

[9] Azarbarmas, M., Emamy, M., Rassizadehghani, J., Alipour, M., Karamouz, M., "Microstructural development of Al-15% Mg_2Si in situ composite with be addition." TMS Annual Meeting, 2011, 2, 829-836.

[10] Mabuchi M, Kubota K, Higashi K., "High strength and high strain rate superplasticity in a Mg–Mg_2Si composite." Scr Metall Mater, 1995, 33, 331–5.

[11] Mabuchi M, Kubota K, Higashi K., "Elevated temperature mechanical properties of magnesium alloys containing Mg_2Si." Mater Sci Technol. 1996, 12, 35–9.

[12] Raghunathan N, Sheppard T., "Fabrication and properties of rapidly solidified magnesium and Mg–Si alloys." Mater Sci Technol. 1990, 6, 629–40.

[13] Frommeyer G, Beer S, Von Oldenburg K., "Microstructure and mechanical properties of mechanically alloyed intermetallic Mg_2Si –Al alloys." Metallkde, 1994, 85, 372–7.

[14] Lu YZ, Wang QD, Zeng XQ, Zhu YP, Ding WJ., "Effects of silicon on microstructure, fluidity, mechanical properties, and fracture behaviour of Mg–6Al alloy." Mater Sci Technol. 2001. 17. 207–14.

[15] Kim JJ, Kim DH, Shin KS, Kim NJ., "Modification of Mg_2Si morphology in squeeze cast Mg–Al–Zn–Si alloys by Ca or P addition." Scr Mater. 1999, 41, 333–40.

[16] Yuan GY, Liu ZL, Wang QD, Ding WJ., "Microstructure refinement of Mg–Al–Zn–Si alloys." Mater Lett. 2002, 56, 53–8.

[17] Yoo MS, Shin KS, Kim NJ. "Effect of Mg_2Si particles on the elevated temperature tensile properties of squeeze-cast Mg–Al alloys." Metall Mater Trans A. 2004, 35, 1629–32.

[18] Flemings MC, Riek RG, Young KP., "The rheology of a partially solid alloy." Metall Trans, 1972, 17, 1925–32.

[19] Wang JL, Su YH., "Structural evolution of conventional cast dendritic and spray-cast non-dendritic structures during isothermal holding in the semi-solid state." Scr Mater. 1997, 37, 2003–7.

[20] Alipour, M., Emamy, M., "Effects of Al-5Ti-1B on the structure and hardness of a super high strength aluminum alloy produced by strain-induced melt activation process." Materials & Design, 2011, 32, 4485-4492.

[21] Alipour, M., Aghdam, B. G., Rahnoma, H. E., Emamy, M., "Investigation of the effect of Al-5Ti-1B grain refiner on dry sliding wear behavior of an Al-Zn-Mg-Cu alloy formed by strain-induced melt activation." Materials & Design, 2013, 46, 766-775.

[22] Alipour, M., Azarbarmas, M., Heydari, F., Alidoost, M., Emamy, M., "The effect of Al-8B grain refiner and heat treatment conditions on the microstructure, mechanical properties and dry sliding wear behavior of an Al-12Zn-3Mg-2.5Cu aluminum alloy." Materials & Design, 2012, 38, 64-73.

[DOI: 10.22068/ijmse.2957]

[23] Haghparast, A., Nourimotlagh, M., Alipour, M., "Effect of the strain-induced melt activation (SIMA) process on the tensile properties of a new developed super high strength aluminum alloy modified by Al5Ti1B grain refiner." Materials Characterization, 2012, 71, 6-18.

[24] karamouz, M., Azarbarmas, M., Emamy, M., Alipour, M., "Microstructure, hardness and tensile properties of A380 aluminum alloy with and without Li additions." Materials Science and Engineering: A, 2013, 582, 409-414.

[25] Mirjavadi, S. S., Alipour, M., Hamouda, A.M.S., Besharati Givi, M.K., Emamy, M., "Investigation of the effect of Al-8B master alloy and strain-induced melt activation process on dry sliding wear behavior of an Al-Zn-Mg-Cu alloy." Materials & Design, 2014, 53, 308-316.

[26] Yang MB, Pan FS, Cheng RJ, Bai L., "Effect of semi-solid isothermal heat treatment on the microstructure of Mg–6A1–1Zn–0.7Si alloy." J Mater Process Technol, 2008, 206, 374–81.

[27] Ma GR, Li XL, Li QF., "Effect of holding time on microstructure of Mg–9Al–1Si alloy during semisolid isothermal heat treatment." Trans Nonferrous Met Soc China, 2010, 20, 430–4.

[28] Zha M, Wang HY, Xue PF, Li LL, Liu B, Jiang QC., "Microstructural evolution of Mg–5Si–1Al alloy during partial remelting." J Alloys Compd, 2009, 472, 18–22.

[29] C. Mondal, A.K. Mukhopadhyay., "On the nature of T(Al2Mg3Zn3) and S(Al2CuMg) phases present in as-cast and annealed 7055 aluminum alloy." Mater. Sci. Eng. A, 2005, 391, 367.

[30] K.J. Burke, "Semi-solid processing of aluminium 7075." PhD thesis. UK, University of Sheffield; 1998.

[31] T.A. Witten, L.M. Sander. "Diffusion-Limited., Phys. Rev. Lett. 1981, 47, 1400.

[32] R.D. Doherty, H.I. Lee, E.A. Feest, "Microstructure of stir-cast metals." Mater. Sci. Eng. A, 1984, 65, 181.

[33] Y. Sirong, L. Dongcheng, N. Kim., "Microstructure evolution of SIMA processed Al2024." Mater Sci Eng A. 2006, 420, 165–170.

[34] Moradi M, Nili-Ahmadabadi M, Poorganji B, Heidarian B, Parsa MH, Furuhara T., "Recrystallization behavior of ECAPed A356 alloy at semi-solid reheating temperature." Mater Sci Eng A. 2010, 527, 4113–4121.

[35] Birol Y., "Thixoforging experiments with 6082 extrusion feedstock." J Alloys Compd. 2008, 455, 178– 185.

[36] M. Alipour, M. Emamy, S.H. Seyed Ebrahimi, M. Azarbarmas, M. Karamouz, J. Rassizadehghani., " Effects of pre-deformation and heat treatment conditions in the SIMA process on properties of an Al–Zn–Mg–Cu alloy modified by Al–8B grain refiner." Mater. Sci. Eng. A, 2011, 528, 4482-4490.

[37] A. Malekan, M. Emamy, J. Rassizadehghani, and M. Malekan., "Effect of Isothermal Holding on Semisolid Microstructure of Al–Mg_2Si Composites." ISRN Metallurgy, 2012, ID 631096, 7.

[38] Sang-Yong, L., Jung-Hwan, L., Young-Seon, L., "Characterization of Al 7075 alloys after cold working and heating in the semi-solid temperature range," Journal of materials processing technology, 2001,111, 42-47.

[39] A.K. Dahle, L. Arnberg, P.A. Tondel and C.J. Paradies, "Effect of grain refinement on the fluidity of two commercial Al-Si foundry alloys". Metallurgical and Materials Transactions A, 1996, 27, 2305-2313.

[40] T.E. Quested, A.L. Greer, J., "The effect of the size distribution of inoculant particles on as-cast grain size in aluminium alloys." Acta Mater. 2004, 52, 3859-3868.

[41] M. Emamy, N. Nemati,A. Heidarzadeh., "The influence of Cu rich intermetallic phases on the microstructure, hardness and tensile properties of Al–15% Mg 2Si composite." Mater. Sci. Eng. A. 2010, 527, 2998–3004.

[42] Mortaza Azarbarmas, Masoud Emamy, Mohammad Alipour, Jafar Rassizadehghani." The effects of boron additions on the microstructure, hardness and tensile properties of in situ Al–15% Mg2Si composite." Materials & Design. 2011, 32, 5049–5054.

[DOI: 10.22068/ijmse.2957]

[43] Jiayue Sun, Chong Li, Xiangfa Liu, Liming Yu, Huijun Li, Yongchang Liu., "Investigation on AlP as the heterogeneous nucleus of Mg_2Si in Al–Mg_2Si alloys by experimental observation and first-principles calculation." Results in Physics, 2018, 8, 146-152.

[44] Hui–Yuan Wang, Feng Liu, Lei Chen, Min Zha, Guo–Jun Liu, Qi–Chuan Jiang., "The effect of Sb addition on microstructures and tensile properties of extruded Al–20Mg_2Si–4Cu alloy." Materials Science and Engineering: A. 2016, 657, 331-338.

[45] M. Emamy, R. Khorshidi, A. Honarbakhsh Raouf, "The influence of pure Na on the microstructure and tensile properties of Al-Mg2Si metal matrix composite." Mater. Sci. Eng. A. 2011, 528, 4337–4342.

[DOI: 10.22068/ijmse.2957]